Cement and Concrete Composites 87 (2018) 1–9

Contents lists available at ScienceDirect

Cement and Concrete Composites

journal homepage: www.elsevier.com/locate/cemconcomp

Investigation of incorporating cinnamaldehyde into Lightweight Aggregate for potential corrosion reduction in cementitious materials

Hajar Jafferji [a, *], Naser P. Sharifi [a], Emily M. Schneider [b], Aaron R. Sakulich [a]

[a] Department of Civil and Environmental Engineering, Worcester Polytechnic Institute, Worcester, MA 01609, USA
[b] Department of Civil and Environmental Engineering, University of Massachusetts Lowell, Lowell, MA 01852, USA

ARTICLE INFO

Article history:
Received 19 October 2016
Received in revised form
22 November 2017
Accepted 28 November 2017
Available online 1 December 2017

Keywords:
Cinnamaldehyde
Lightweight Aggregate
Corrosion mitigation
Deterioration of infrastructures

ABSTRACT

Each year, corrosion of concrete results in billions of dollars' worth in damage. Cinnamaldehyde, a bioactive agent, can mitigate the corrosion of metals and potentially protect rebar within concrete. However, it cannot be incorporated into concrete during mixing since it negatively effects the hydration reaction between cement and water. To avoid these undesirable effects while keeping anti-corrosive properties in a cementitious mixture, an innovative approach through the use of Lightweight Aggregate (LWA) was taken. The experimental cinnamaldehyde-LWA mortar showed reduced compressive strength, heat evolution, and rebar pullout bond stress, but promising results regarding chloride threshold level and sorptivity.

1. Introduction

Concrete can prematurely deteriorate due to the corrosion of reinforcing steel. This is particularly critical since concrete is a staple building material worldwide of which nearly five billion tonnes is produced annually – approximately 1 tonne (1.102 tons) of concrete per person each year [1]. When aggressive media such as chloride ions from deicing salts or seawater diffuse through concrete, they can depassivate reinforcing steel and result in the production of expansive products, mainly iron oxides (rust). This buildup of rust can crack the concrete and lead to spalling [2]. Although there are numerous mitigation methods on the market today (e.g. epoxy coated rebar, waterproofing membranes, cathodic protection, etc.), $100 billion is still expended annually on corrosion related damage [3–5]. Therefore, novel methods for corrosion prevention are necessary.

This experimental program takes an innovative approach to corrosion mitigation. Cinnamaldehyde, the essential oil of cinnamon and a derivative of cinnamon bark, is a natural bioactive agent. This bioactive agent is commonly used in food for flavoring and in the medical field as a way to help those with diabetes [6]. However, it has also been shown to mitigate the corrosion of steel by forming a protective film on the surface of metals [7–9]. One drawback is that when cinnamaldehyde is included in a cementitious matrix it can coat cement particles and prevent the hydration of the cement, therefore causing a reduction of its compressive strength [10,11]. One way that cinnamaldehyde can be incorporated without interfering with the properties of concrete is by encapsulation in Lightweight Aggregate (LWA) [12,13]. Conventionally, LWA is presoaked with water and used to prevent early age cracking, a method known as 'internal curing' [14]. Over time, hydration of the cement causes an internal drop in humidity, causing the liquid absorbed by the LWA to be released in order to attain pressure equilibrium. Thus, by soaking the LWA in cinnamaldehyde, the cinnamaldehyde will be encapsulated within the LWA allowing it to be transported into the cementitious matrix and can be released once the early-age properties have developed [14]. After release, the cinnamaldehyde can diffuse towards the reinforcing steel and coat the steel to protect it against corrosion.

This research program further investigates a previous study by providing other considerations as well as additional experimental research [25]. This study investigates the potential impacts that cinnamaldehyde has on the cementitious matrix, and the efficiency of LWA as an encapsulation method for corrosion prevention agents. In doing so, six tests were carried out: compressive strength, to determine the mechanical effects of cinnamaldehyde incorporation; isothermal calorimetry, to examine hydration

* Corresponding author. Department of Civil and Environmental Engineering, Worcester Polytechnic Institute, 100 Institute Rd., Worcester, MA 01609-2280, USA.
E-mail address: hajar@wpi.edu (H. Jafferji).

https://doi.org/10.1016/j.cemconcomp.2017.11.022
0958-9465/

Table 1
Mix proportioning.

Mix number		Mix 1		Mix 2		Mix 3	
		Volume (cm^3)	Mass (g)	Volume (cm^3)	Mass (g)	Volume (cm^3)	Mass (g)
Sand (Total)		1375.0	3588.8	1046.7	2731.9	1046.7	2731.9
LWA (Total)		N/A[a]	N/A	328.3	492.5	328.3	492.5
#8	Sand	412.5	1076.6	314.0	819.6	314.0	819.6
	LWA	N/A	N/A	98.5	147.7	98.5	147.7
#16	Sand	343.8	897.2	261.7	683.0	261.7	683.0
	LWA	N/A	N/A	82.1	123.1	82.1	123.1
#30	Sand	275.0	717.8	209.3	546.4	209.3	546.4
	LWA	N/A	N/A	65.7	98.5	65.7	98.5
#50	Sand	206.3	538.3	157.0	409.8	157.0	409.8
	LWA	N/A	N/A	49.2	73.9	49.2	73.9
#100	Sand	137.5	358.9	104.7	273.2	104.7	273.2
	LWA	N/A	N/A	32.8	49.2	32.8	49.2
Mixing water		585.4	585.4	585.4	585.4	585.4	585.4
Cement		464.6	1463.5	464.6	1463.5	464.6	1463.5
Internal water		N/A	N/A	86.2	86.2	N/A	N/A
CA[b]		N/A	N/A	N/A	N/A	86.2	90.5

[a] Not Applicable.
[b] Cinnamaldehyde.

kinetics; sorptivity and diffusion of sodium chloride (NaCl) tests to determine transport properties; measurement of chloride threshold level; and rebar pullout.

2. Materials and methods

[1]Three mortar mixes were produced and tested. Mix 1 served as the control and was composed of local sand, ASTM C150 Type I/II cement, and water. The two other mixes (Mix 2 and Mix 3) were experimental and consisted of the same components as Mix 1, but included a partial replacement of the sand with presoaked LWA. Mix 2 contained water-LWA and Mix 3 contained cinnamaldehyde-LWA. The concentration of cinnamaldehyde (C_9H_8O) was provided by the manufacturer as 132.16 g/mol. Each mix had a water:cement ratio of 0.4 (not including the water stored within the LWA), and a 55 vol% of aggregate as shown in Table 1. It should be mentioned that these are arbitrary percentages in the acceptable and conventional range for mortar mix proportioning; and since they are the same for all the mixes, they do not affect the results. LWA was soaked in water for at least 24 h in a sealed container. After 24 h, the presoaked LWA was then incorporated into Mix 2 in a Saturated Surface Dry (SSD) state. The same method was used for encapsulating cinnamaldehyde in the LWA for Mix 3.

The LWA was commercially available expanded shale (Northeast Solite Corporation) with an absorption capacity of water of 17.5 wt% (as determined by the manufacturer). Mixes that included LWA involved a partial replacement of the local sand with LWA on a volumetric basis in order to retain the same particle size distribution as the sand. The amount of LWA needed for the mixes was calculated by Ref. [14]:

$$M_{LWA} = \frac{C_f \times CS \times \alpha_{max}}{S \times \Phi_{LWA}} \quad (1)$$

where M_{LWA} is the mass of dry LWA per unit volume of mortar (kg/m^3); C_f is the cement factor of the mortar (kg/m^3); CS is the chemical shrinkage of the cement (g of water/g of cement) (determined using ASTM C1608 [15] – Fig. 1); α_{max} is maximum degree expected of hydration of cement (dimensionless); S is the saturation degree of LWA (dimensionless); and Φ_{LWA} is the absorption capacity of the LWA (g water/g dry LWA) (Table 2).

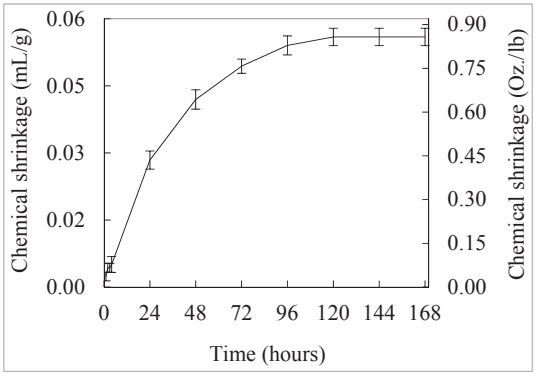

Fig. 1. Chemical shrinkage.

In order to investigate the chemistry of the mortars, Fourier Transformation Infrared Spectroscopy (FTIR) and X-ray Diffraction (XRD) were used for the identification of chemical species. The microstructures of the mortars, focusing on the Interfacial Transition Zone (ITZ), were further examined by Scanning Electron Microscopy (SEM).

The compressive strengths of all mixes were determined in accordance with ASTM C109 [16]. Once mixed, the mortar (at least three samples per mix) was immediately placed and tamped into 2 in. (50.8 mm) cube molds, sealed in a plastic bag, and stored in a fog room. Samples were demolded after 24 h, placed back into the fog room to cure, and tested at ages of 3, 7, 28, and 91 d.

Isothermal calorimetry was used to assess the hydration kinetics of the mortars. The heat flows of the mortars (two samples of each mix) were evaluated during the initial 24 h of hydration. Once the mortars were mixed, the appropriate amount was immediately placed in an ampoule and sealed. Heat flow was normalized by cement content.

Sorptivity tests were conducted following ATSM C1585 [17]. Mortar was placed into 4 × 2 in. (101.6 × 50.8 mm) cylinders, stored in a fog room, demolded after 24 h and placed back in the fog room to cure for 28 d (three samples per mix). On day 28, the samples

[1] Certain commercial equipment, instruments, or materials are identified in this report in order to specify the experimental procedure adequately. Such identification is not intended to imply recommendation or endorsement, nor is it intended to imply that the materials or equipment identified are necessarily the best available for the purpose.

Table 2
Values used to calculate M_{LWA}.

Variable	Value
C_f	585 kg/m^3
CS	0.056 ml/g
α_{max}	1
S	0.95
Φ_{LWA}	0.175

were removed from the fog room and placed in an oven at 221 °F (105 °C) to dry for 24 h. Once removed from the oven and cooled, the circumference of each cylinder was sealed using duct tape in order to ensure unidirectional sorption. The samples were then placed on supports at the bottom of an enclosed plastic tank. Water was filled into the tank such that it was 0.08 ± 0.04 in. (2 ± 1 mm) above the bottom of the sample; the water level was maintained throughout the experiment. Absorption, *I*, was calculated by:

$$I = \frac{m_t}{a \times d} \quad (2)$$

where I is the absorption (mm); m_t is the change in mass at time *t* (g); *a* is the exposed area of the sample (mm^2); and *d* is the density of water (g/mm^3).

Both the initial and secondary rates of water sorptivity were identified as the slopes of the lines of the absorption plotted against the square root of time. To characterize initial sorptivity, the masses of the sample were taken at 60 s, 5 min, 10 min, 20 min, 30 min, 60 min, and every hour for the following 6 h. The secondary rate of absorption is found in the same manner as the initial rate but at later ages. Masses were recorded once every ~24 h for a total of 7 d.

The diffusion of NaCl through these mortars was examined. Mortar (three samples per mix) was placed in 4 × 2 in. (101.6 × 50.8 mm) cylinder molds. After 28 d curing, the cylinders were each immersed in a 5 wt% NaCl solution stored in a sealed plastic tank for 3 months. The samples were removed from the solution, split lengthwise, and sprayed with silver nitrate ($AgNO_3$) [18,19]. The silver nitrate changes the color of the mortar such that where there is a concentration of chloride ions, the mortar is lighter in color (normally around the top, bottom, and sides). A program developed by the NIH (ImageJ) was used to determine color variations and calculate the area through which the chloride had diffused (Fig. 2).

Additionally, the Chloride Threshold Level (CTL) was measured. The CTL can be described as the chloride content at the depth of the steel such that it breaks down the passive layer and initiates corrosion [20]. In order to determine the CTL, two steps had to take place: corrosion initiation and measurement of the chloride content. In order to initiate corrosion, an Accelerated Corrosion Test (ACT) was carried out [21,22]. The ACT consisted of a plastic tank containing 5 wt% NaCl solution, two stainless steel plates (the cathodes), and a 30 V DC power supply to accelerate the corrosion (Fig. 3). Mortar was placed into 4 × 8 in. (101.6 × 203.2 mm) cylinders with a ½ in. (12.7 mm) wire-brushed steel rebar embedded in the center (three samples for each mix). To avoid crevice corrosion, epoxy was coated at the top of the cylinder where the rebar exits the mortar. After 28 d of curing, the samples were placed into the ACT and a data logger recorded the current. Once a sharp increase in current (indicating the initiation of corrosion) was observed, the test was immediately terminated. While it is known that accelerated tests do not resemble field conditions, an ACT was used as a method for proof of concept. To determine the chloride content, Ion Chromatography (IC) was used. The corrosion-initiated cylinders were split lengthwise and a sample of mortar was taken at four different depths (Fig. 4): from the surface to ½ in. (12.7 mm)

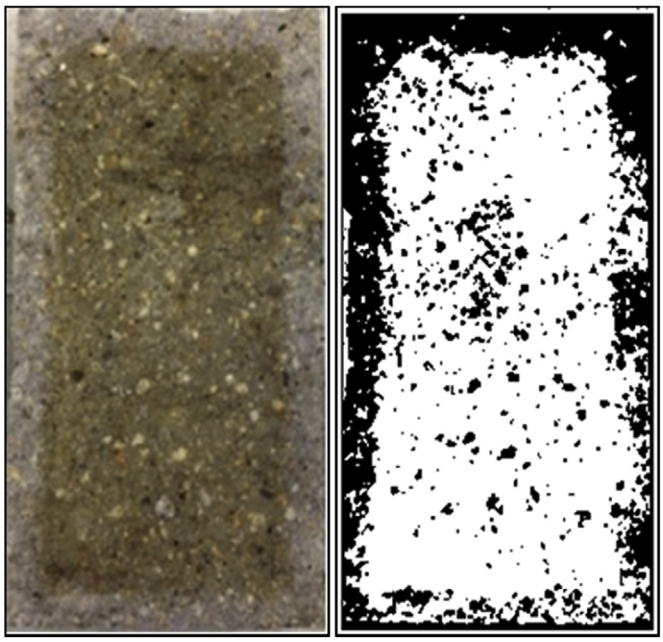

Fig. 2. Mortar sample sprayed with silver nitrate ($AgNO_3$).
The light gray around sample indicates the depth of chloride ingress (left),
The binarization of the sample using ImageJ where the black indicates chloride ingress (right).

deep into the sample; 1 ½ in. (38.1 mm); 2 in. (50.8 mm); and along the length of the mortar-rebar interface. These samples were obtained with a masonry drill. 1 g of powder was added to a 150 ml beaker which was then filled with 100 ml of deionized water and left to soak for about 15 h. After soaking, the samples were heated on a hotplate at 184 °F (84.4 °C) for 3 h. The solution was then filtered using a No. 4 filter into a 100 ml flask and washed with deionized water to fill the 100 ml. The concentration of chloride ions in the original sample was determined by:

$$Cl = \frac{R \times Fl}{W} \quad (3)$$

where Cl is the concentration of chloride ions in the original sample (mg/g); R is the concentration of chloride ions in the sample from the ion chromatograph (mg/l); Fl is the volume of the flask containing undiluted sample (l); and W is the weight of the original powdered sample (g).

Finally, to identify if the experimental mixes (Mix 2 and mix 3) interfered with the bond strength between mortar and rebar, rebar pullout tests were conducted [23]. Samples were prepared by placing mortar into 6 × 12 in. (152.4 × 304.8 mm) cylinders and embedding a ¾ in. (19.1 mm) wire-brushed rebar of 3 ft. (91.4 cm) in the center. To ensure perpendicular alignment a jig was made to hold the rebar in place. Once cured for 28 d, the samples (three for each mix) were placed on the top crosshead of a load frame where the rebar ran through the lower crosshead and was secured by jaws (Fig. 5). A shim was put between the top of the tensile frame and the cylinder to reduce the effects of eccentricity. A displacement rate of 0.1 in/min was used.

3. Results and discussion

Mixes containing presoaked LWA resulted in lower compressive strengths (Fig. 6). Mix 2, which contained water-LWA, resulted in reduced strengths when compared to the control by 4% at 3 d and

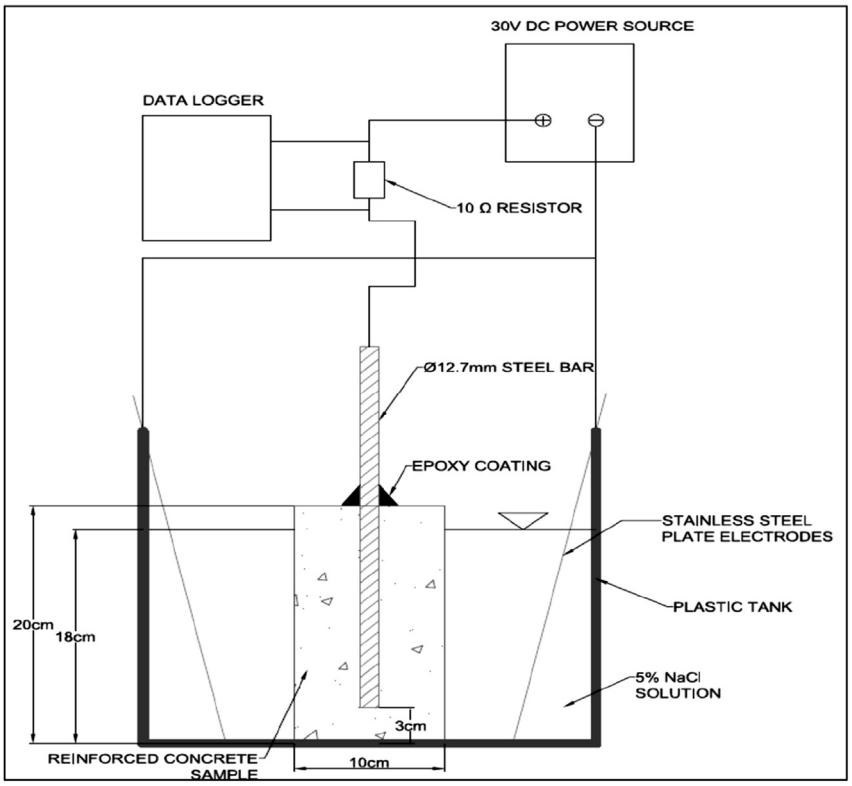

Fig. 3. Schematic of accelerated corrosion test (ACT) [25].

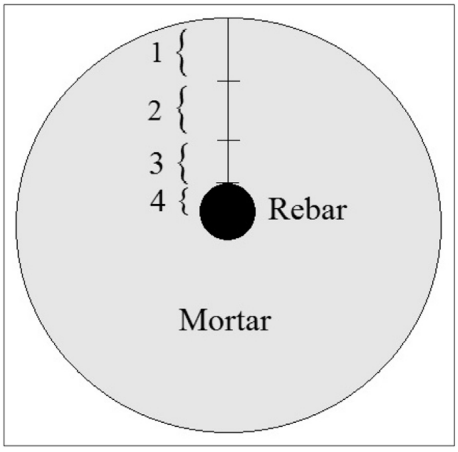

Fig. 4. A top view of the sample section along with the four depths that were drilled out and tested for chloride content through ion chromatography. 1) is the powdered mortar collected from the depth of surface to ½ in.; 2) is the powdered mortar collected from the depth of ½ in. to 1 ½ in.; 3) is the powdered mortar collected from the depth of 1 ½ in. to 2 in.; 4) is the powdered mortar collected along the length of the mortar-rebar interface.

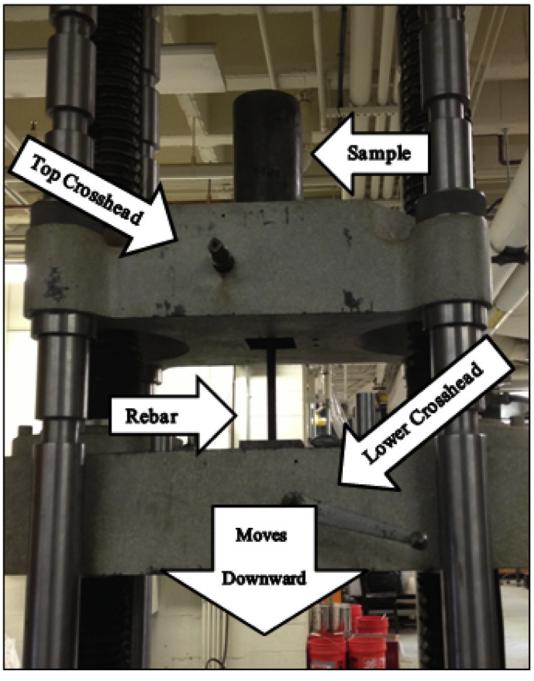

Fig. 5. Rebar pullout setup.

7 d; 8% at 28 d; and 7% at 91 d. This decrease in strength is likely due to the weak nature of the porous LWA [24]. When using LWA to encapsulate cinnamaldehyde (Mix 3) larger reductions in strength were observed. Compressive strength decreased by 31% at 3 d, 33% at 7 d, 40% at 28 d, and 41% at 91 d, indicating that either a surplus of cinnamaldehyde remains on the surface of the LWA (which may prevent the formation of mechanical bonds between LWA and the cementitious matrix), or LWA is releasing the cinnamaldehyde early enough to interfere with the hydration reactions by coating cement particles and inhibiting hydration. A previous study observed similar results when incorporating cinnamaldehyde-LWA in mortars [25].

The FTIR spectra of the three mortar mixes consisted of six similar bands: a band at 600 cm^{-1} due to Si-O vibrations; a band at

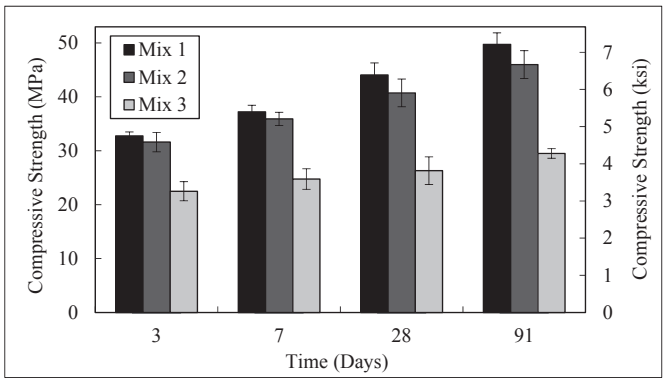

Fig. 6. Compressive strength of mortars at ages 3, 7, 28, and 91 d.

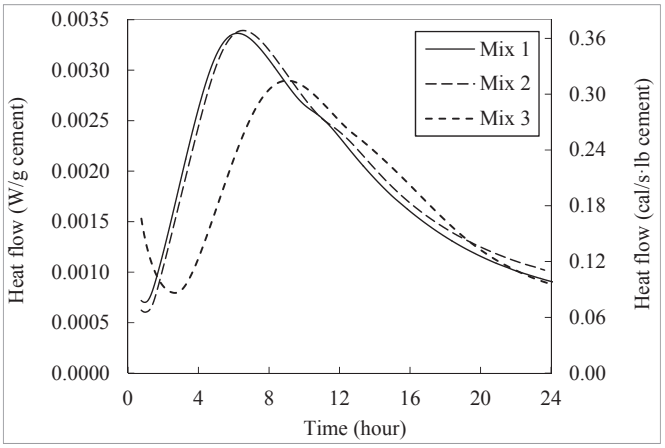

Fig. 9. Isothermal calorimetry.

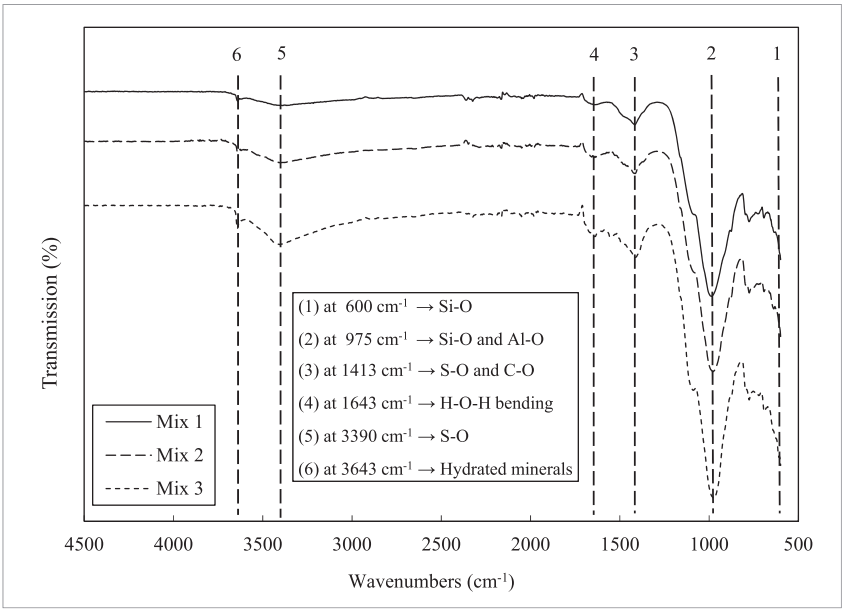

Fig. 7. FTIR spectra of the mortars.

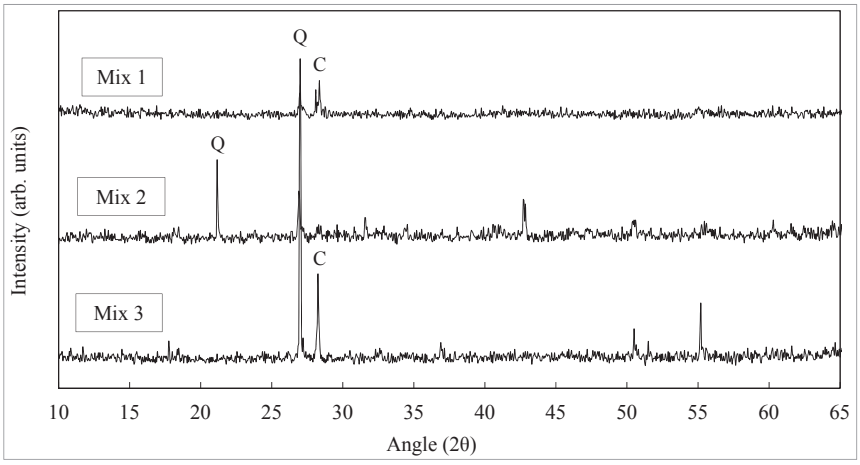

Fig. 8. XRD diffractograms of mortars. Notes: Q is quartz and C is calcite.

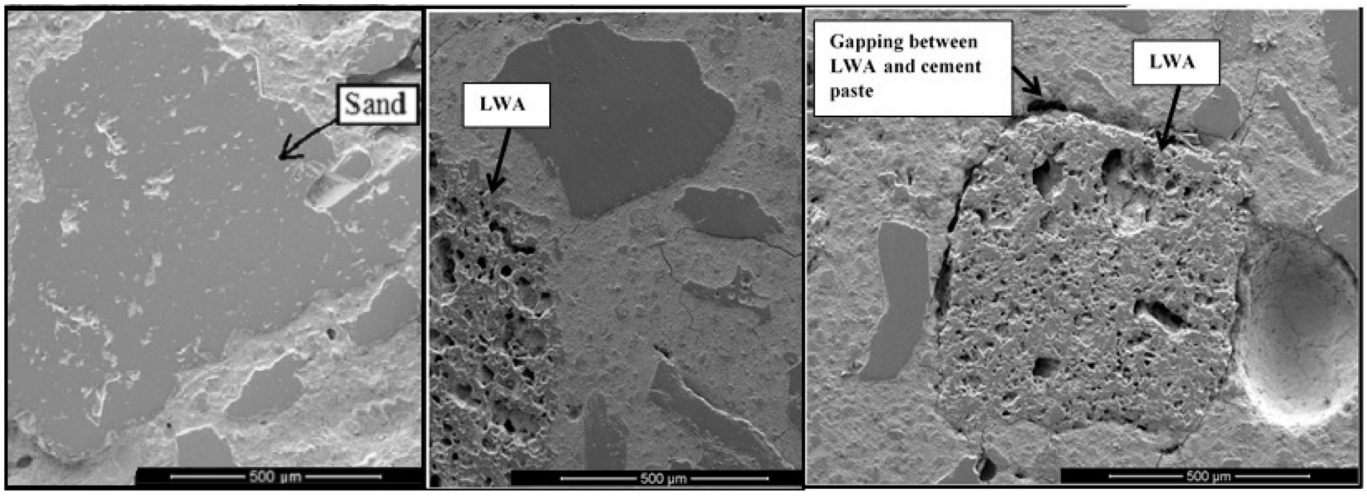

Fig. 10. SEM image on left is Mix 1 (control), which does not contain LWA. SEM image in the middle is Mix 2. No apparent ITZ is observed around the LWA. The SEM image on the right shows how Mix 3 produces a gapping space between the LWA and the cement paste. This can be a cause of the reduction in compressive strength.

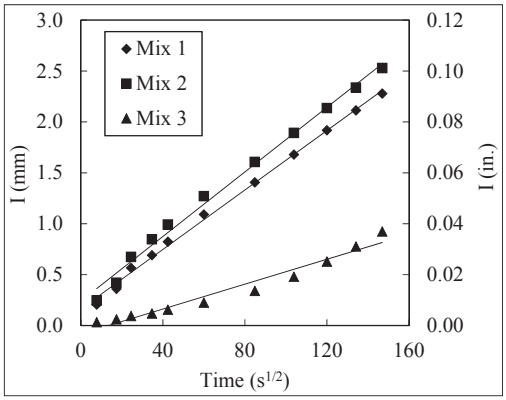

Fig. 11. Initial rate of water absorption.

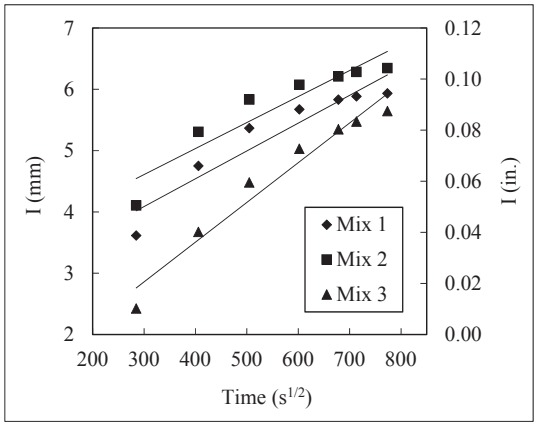

Fig. 12. Secondary rate of water absorption.

975 cm^{-1} due Si-O and Al-O vibrations; a band at 1413 cm^{-1} due to S-O and C-O vibrations; a band at 1643 cm^{-1} due to H-O-H bending; a band at 3390 cm^{-1} due to S-O; and a band 3643 cm^{-1} due to hydrated minerals (Fig. 7). XRD identified traces of crystalline quartz and calcite in each of the three mortar mixes (Fig. 8). The results of the FTIR and XRD experiments are similar to those reported elsewhere in literature [26,27]. The similarity in FTIR spectra and x-ray diffractograms indicate that any potential effects on mechanical properties in mortars containing cinnamaldehyde are unlikely to be due to the formation of new chemical species.

Hydration is an exothermic reaction and the hydration kinetics of the mixes were observed by isothermal calorimetry (Fig. 9). Mix 2 displayed a slight acceleration when compared with the control (Mix 1). This has been previously observed and is due to additional hydration provided by absorbed water [28]. However, the hydration of Mix 3 was somewhat retarded, with a 14% reduction of heat flow compared to the control. A rightward shift is also evident, indicating a significant delay in hydration.

Microscopic investigation of the mortars suggests that the addition of cinnamaldehyde interferes with the development of the cementitious matrix. Gapping around the ITZ of the LWA was observed in Mix 3 (Fig. 10). Gaps between cement paste and LWA may be due to the cinnamaldehyde remaining on the surface of the LWA and therefore preventing the adhesion of the paste to the LWA, which is a possible explanation for the reduction of compressive strength. Such gapping is not seen around the ITZ of the LWA in Mix 2; this denser microstructure was also observed in a study of internal curing by Bentz and Stutzman [29].

The initial rates of absorption follow a linear relationship, with a correlation coefficient of 0.98 or greater (Fig. 11). The sorptivity coefficient of Mix 2 was slightly larger when compared to the control within the first 6 h (Table 3). Since sorptivity relates to the ability of the pore structure to absorb liquid by capillary forces, this

Table 3
Regression equations of initial rate of water absorption.

Sample	Regression equation	Correlation coefficient	Sorptivity coefficient ($mm/\sqrt{s}$)
Mix 1	y = 0.0146x + 0.163	0.998	0.0146
Mix 2	y = 0.0159x + 0.240	0.997	0.0159
Mix 3	y = 0.0061× - 0.082	0.98	0.0061

may explain the reason that Mix 2 has the greatest initial sorptivity [30]. Once the LWA releases the stored liquid, the pores of the LWA are empty and therefore can absorb water. However, the addition of cinnamaldehyde (Mix 3) led to a lower initial sorptivity coefficient compared to the control. This may be due to cinnamaldehyde filling the pores of the cementitious matrix through the initial phases of sorptivity.

However, the secondary rate of water absorption for Mix 1 and Mix 2 did not follow a linear relationship, with correlation coefficients of 0.945 and 0.934, respectively (Fig. 12). Ghafari et al. observed similar nonlinear coefficients when testing the sorptivity of ultra-high performance concrete; the nonlinear results were used as an approximation of sorptivity [31]. The results of the regression equations were used for estimation of the secondary

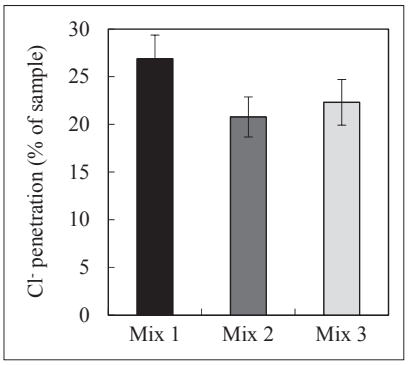

Fig. 14. Chloride penetration of split cylinders in terms of the percentage of the mortar sample.

Table 4
Regression equations for secondary rate of water absorption.

Sample	Regression equation	Correlation coefficient	Sorptivity coefficient ($mm/\sqrt{s}$)
Mix 1	$y = 0.0045x + 2.7285$	0.945	0.0045
Mix 2	$y = 0.0042x + 3.3381$	0.934	0.0042
Mix 3	$y = 0.0065x + 0.9166$	0.98	0.0065

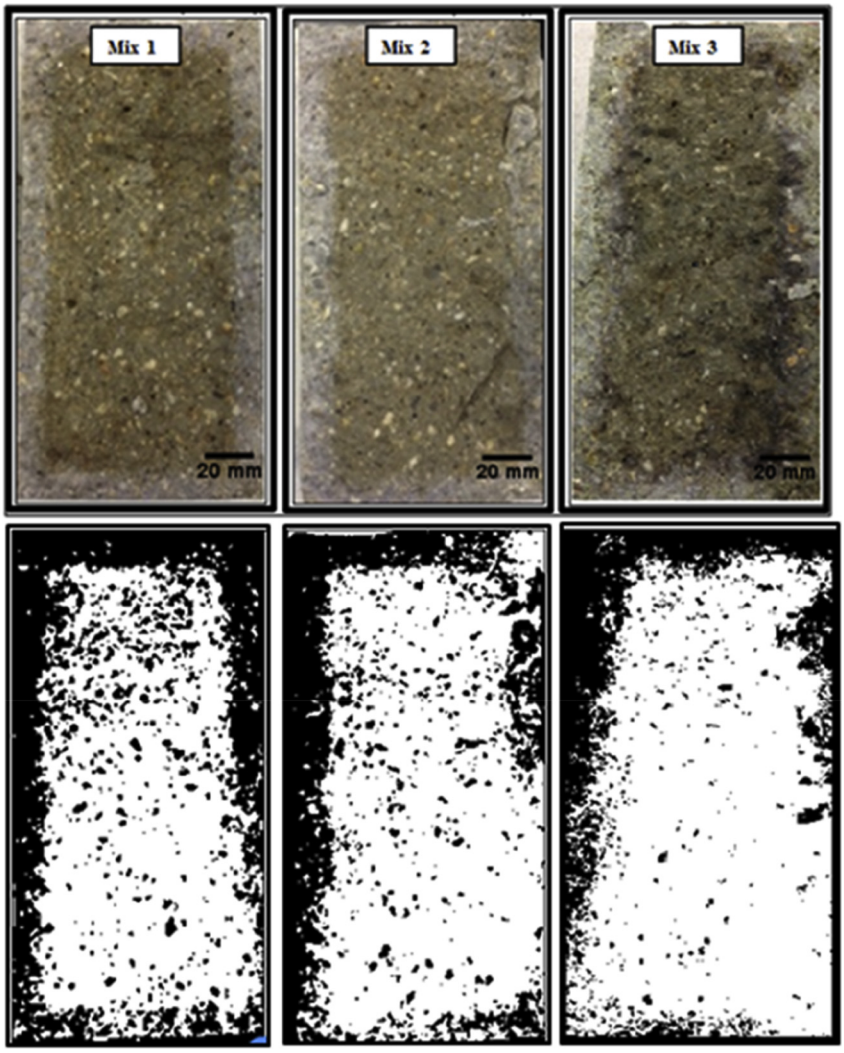

Fig. 13. Samples of cylinders split lengthwise and sprayed with silver nitrate after exposed to NaCl solution bath for 3 months (top row of images) along with the binarization of each sample (bottom row).

rate of sorptivity, despite being nonlinear, (Table 4). Between 1 d and 7 d, the sorptivity coefficients of Mix 1 and Mix 2 decreased, a trend observed elsewhere in the literature [30]. However, the secondary rate of water absorption for Mix 3 increased slightly. This may be due to the cinnamaldehyde fully emptying out of the LWA pores, suggesting that cinnamaldehyde is exiting the LWA pores at a faster rate when compared with the water in Mix 2.

In terms of NaCl diffusion, the area (measured in percentage) through which chloride penetrated Mix 2 was 23% less when compared with Mix 1 (Fig. 13). This may be due to the LWA creating a denser ITZ microstructure due to additional hydration [32]. It should be mentioned that based on the results of another study in which similar LWA was incorporated in the mortar, the incorporation of LWA does not produce alternative phases in the media and does not change the crystal structure of the mortar. Therefore, the LWA does not have a chemical side effect on the mortar [33]. The diffusion of NaCl through Mix 3 was 17% less than Mix 1, possibly due to the cinnamaldehyde filling the pores within the cementitious matrix and altering the transport properties of the pore solution (Fig. 14).

Table 5
Time to corrosion initiation of samples.

Sample	Average (day)	Standard Deviation (day)
Mix 1	2.9	±0.08
Mix 2	2.9	±0.08
Mix 3	32.1	±18.4

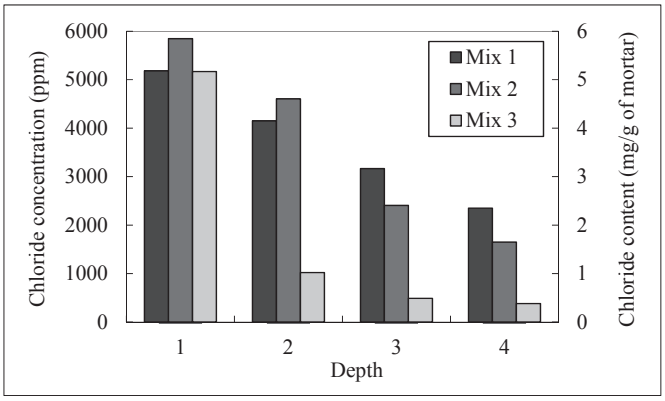

Fig. 15. Chloride concentration at varying depth within the lollipop sample. The depths refer to Fig. 4 where: (1) is the powdered mortar collected from the depth of surface to ½ in.; (2) is the powdered mortar collected from the depth of ½ in. to 1 ½ in.; (3) is the powdered mortar collected from the depth of 1 ½ in. to 2 in.; (4) is the powdered mortar collected along the length of the mortar-rebar interface.

The times to initiation of corrosion of the samples are listed in Table 5. The resulting times for corrosion initiation of Mixes 1 and 2 were roughly similar, however, it took Mix 3 roughly 91% longer for the corrosion initiation process to begin. This has previously been observed and is likely due to the cinnamaldehyde creating a protective film on the reinforcing steel as well as slowing the ingress of chloride [25]. The chloride concentrations at the four depths (surface to ½ in. (12.7 mm), 1 ½ in. (38.1 mm), 2 in. (50.8 mm), and along the length of the mortar-rebar interface) were determined by ion chromatography (Fig. 15). Mix 2 has a slightly greater chloride concentration from the surface to ½ in. (12.7 mm) and 1 ½ in. (38.1 mm) than the control (Mix 1) but lower concentrations at 2 in. (50.8 mm) and along the length of the mortar-rebar interface. Mix 3 has the lowest concentration of chloride at all depths. The lower chloride concentrations combined with the lengthened time to corrosion indicates that the cinnamaldehyde increases the CTL of the sample. Due to the sensitivity of the test, large standard deviations were observed and were omitted from the figure for clarity purposes – as such, the values should be taken as only potentially indicative of an increase in the CTL.

The bond strengths between the matrix and rebar were determined for each mix. Results of the rebar pullout test show that Mix 2 has the greatest bond strength (Fig. 16). The failure pattern of Mix 2 also reveals gradual failure, with plateau-like behavior, prolonging the time to failure. This may be due to the denser microstructure of the mix. Mix 3 yields the lowest bond stress with a sharp failure mode (as opposed to the plateaus observed in Mix 2) due to the cinnamaldehyde coating the rebar. Further studies are needed to fully determine the reasons for such failures, and it is likely that the reduced rebar/matrix bond strength would have to be overcome before this system could have any practical applications.

4. Conclusions

A preliminary study on incorporating cinnamaldehyde in

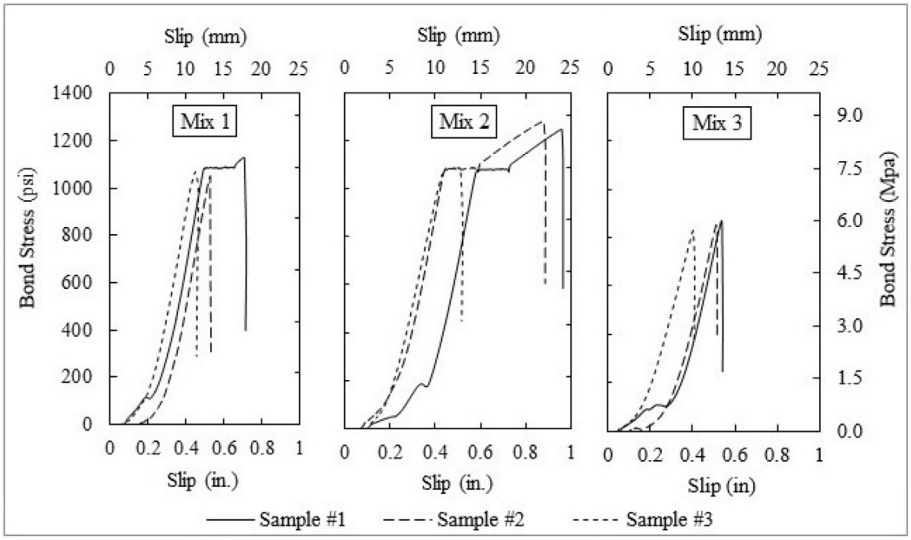

Fig. 16. Rebar pullout results plotted as bond stress over slip.

cementitious systems through encapsulation in LWA has been carried out. The experimental program aimed to investigate the novel cinnamaldehyde-LWA in terms of corrosion mitigation and the impact on the cementitious properties. Although properties, such as the mechanical properties, of the experimental mortar were impacted, this technology is promising due to the significantly prolonged corrosion resistance observed by the inclusion of the cinnamaldehyde-LWA under accelerated corrosion conditions. Future research should include a study on the substantial increase in corrosion life when using the cinnamaldehyde-LWA. Moreover, surface analyses such as SEM imaging should be carried out in order to confirm the presence of cinnamaldehyde on the surface of the rebar. Additional research on including LWA as a transport mechanism for corrosion mitigation agents without affecting the hydration should be conducted.

Acknowledgements

Parts of this research were funded with a seed grant from the American Concrete Institute's Concrete Research Council [CRC 74]. Emily Schneider was supported by funds from a National Science Foundation Research Experience for Undergraduates site [Award #1359064]. The authors would like to thank Northeast Solite Corporation for providing lightweight aggregate.

References

[1] E.J. Garboczi, D.P. Bentz, Multi-Scale Picture of Concrete and its Transport Properties: Introduction for Non-Cement Researchers 5900, National Institute of Standards and Technology Internal Report, 1996.
[2] H. Böhni, "Corrosion in Reinforced Concrete Structures, Elsevier, 2005, p. 2.
[3] J.P. Broomfield, Corrosion of Steel in Concrete: Understanding, Investigation and Repair, CRC Press, 2002, pp. 201–212.
[4] F. Li, Y. Yuan, C.-Q. Li, Corrosion propagation of prestressing steel strands in concrete subject to chloride attack, Constr. Build. Mater. 25 (10) (May 2011) 3878–3885.
[5] Z.J. Chen, Effect of Reinforcement Corrosion on the Serviceability of Reinforced Concrete Structures, MSc thesis, Department of Civil Engineering, University of Dundee, UK, 2004.
[6] P.S. Babu, S. Prabuseenivasan, S. Ignacimuthu, Cinnamaldehyde—a potential antidiabetic agent, Phytomedicine 14 (1) (October 2006) 15–22.
[7] F. Growcock, W. Frenier, Kinetics of steel corrosion in hydrochloric acid inhibited with trans-Cinnamaldehyde, J. Electrochem. Soc. 135 (4) (April 1988) 817–823.
[8] N.A. Negm, M.A. Yousef, S.M. Tawfik, Impact of synthesized and natural compounds in corrosion inhibition of carbon steel and aluminium in acidic media, Recent Pat. Corros. Sci. 3 (1) (May 2013) 58–68.
[9] K.A. Rieger, J.D. Schiffman, Electrospinning an essential oil: cinnamaldehyde enhances the antimicrobial efficacy of chitosan/poly (ethylene oxide) nanofibers, Carbohydr. Polym. 113 (July 2014) 561–568.
[10] H. Jafferji, G.T. Keohane, J.D. Schiffman, A.R. Sakulich, Preliminary investigations of essential oils as corrosion inhibitors in steel reinforced cementitious systems, in: Proceeding of the Thrity-fifth Conference on Cement Microscopy, USA, April-May 2013, pp. 40–48.
[11] H. Jafferji, A.R. Sakulich, Impact of corrosion inhibitors on design, in: Proceedings of the 2nd International Workshop on Design in Civil and Environmental Engineering, USA, June 2013, pp. 95–100.
[12] D.P. Bentz, R. Turpin, Potential applications of phase change materials in concrete technology, Cem. Concr. Compos. 29 (7) (August 2007) 527–532.
[13] A.R. Sakulich, D.P. Bentz, Increasing the service life of bridge decks by incorporating phase-change materials to reduce freeze-thaw cycles, J. Mater. Civ. Eng. 24 (8) (August 2012) 1034–1042.
[14] D.P. Bentz, W.J. Weiss, Internal Curing: a 2010 State-of-the-art Review, US Department of Commerce, National Institute of Standards and Technology, NISTIR 7765, February 2011.
[15] ASTM C1608-12, Standard Test Method for Chemical Shrinkage of Hydraulic Cement Paste, ASTM International, West Conshohocken, PA, 2012.
[16] ASTM C109-13 Compressive Strength of Hydraulic Cement Mortars (Using 2-in. Or [50-mm] Cube Specimens). ASTM International: West Conshohocken, PA.
[17] ASTM C1585-13 Standard Test Method for Measurement of Rate of Absorption of Water by Hydraulic-cement Concretes. ASTM International: West Conshohocken, PA.
[18] V. Baroghel-Bouny, P. Belin, M. Maultzsch, D. Henry, AgNO3 spray tests: advantages, weaknesses, and various applications to quantify chloride ingress into concrete. Part 1: non-steady-state diffusion tests and exposure to natural conditions, Mater. Struct. 40 (8) (April 2007) 759–781.
[19] V. Baroghel-Bouny, P. Belin, M. Maultzsch, D. Henry, AgNO3 spray tests: advantages, weaknesses, and various applications to quantify chloride ingress into concrete. Part 2: non-steady-state migration tests and chloride diffusion coefficients, Mater. Struct. 40 (8) (April 2007) 783–799.
[20] K.Y. Ann, H.-W. Song, Chloride threshold level for corrosion of steel in concrete,", Corros. Sci. 49 (11) (June 2007) 4113–4133.
[21] E. Güneyisi, T. Özturan, M. Gesoğlu, A study on reinforcement corrosion and related properties of plain and blended cement concretes under different curing conditions, Cem. Concr. Compos. 27 (4) (April 2005) 449–461.
[22] E. Güneyisi, M. Gesoğlu, F. Karaboğa, K. Mermerdas, Corrosion behavior of reinforcing steel embedded in chloride contaminated concretes with and without metakaolin, Compos. Part B Eng. 45 (1) (February 2013) 1288–1295.
[23] G. Chen, J. Volz, R. Brow, D. Yan, S. Reis, C. Wu, F. Tang, C. Werner, X. Tao, Coated Steel Rebar for Enhanced Concrete-Steel Bond Strength and Corrosion Resistance, 2010. No: NUTC R236.
[24] D.P. Bentz, Internal curing of high-performance blended cement mortars, ACI Mater. J. 104 (4) (July 2007) 408–414.
[25] H. Jafferji, A.R. Sakulich, J.D. Schiffman, Preliminary study on mitigating steel reinforcement corrosion with bioactive agent, Cem. Concr. Compos. 69 (May 2016) 9–17.
[26] H. Biricik, N. Sarier, Comparative study of the characteristics of nano silica -, silica fume - and fly ash - incorporated cement mortars, Mater. Res. 17 (3) (May-June 2014) 570–582.
[27] E.J.P.d. Miranda Júnior, H.d.J.C.L. Bezerra, F.S. Politi, A.E.M. Paiva, Increasing the compressive strength of Portland cement concrete using flat glass powder, Mater. Res. 17 (August 2014) 45–50.
[28] D.P. Bentz, Influence of internal curing using lightweight aggregates on interfacial transition zone percolation and chloride ingress in mortars, Cem. Concr. Compos. 31 (5) (May 2009) 285–289.
[29] D.P. Bentz, P.E. Stutzman, Internal curing and microstructure of high-performance mortars, ACI Spec. Publ. 256 (October 2008) 81–90.
[30] T.Y. Lo, H.Z. Cui, A. Nadeem, Z.G. Li, The effects of air content on permeability of lightweight concrete, Cem. Concr. Res. 36 (10) (October 2006) 1874–1878.
[31] E. Ghafari, H. Costa, E. Júlio, A. Portugal, L. Durães, The effect of nanosilica addition on flowability, strength and transport properties of ultra high performance concrete, Mater. Des. 59 (July 2014) 1–9.
[32] D.P. Bentz, K.A. Snyder, M.A. Peltz, Doubling the service life of concrete structures. II: performance of nanoscale viscosity modifiers in mortars, Cem. Concr. Compos. 32 (3) (March 2010) 187–193.
[33] Naser P. Sharifi, et al., Application of lightweight aggregate and rice husk ash to incorporate phase change materials into cementitious materials, J. Sustain. Cement-Based Mater. 5.6 (2016) 349–369.

Hajar Jafferji is a Ph.D. candidate at Worcester Polytechnic Institute (WPI) in the Civil and Environmental Engineering Department. She received her B.S. and M.S. from WPI in 2011 and 2012, respectively. Her research interests include prevention of premature deterioration of infrastructure.

Naser P. Sharifi is a Ph.D. candidate in the Department of Civil and Environmental Engineering at Worcester Polytechnic Institute (WPI). He received his BSc. from Isfahan University of Technology in 2009, and his MSc. from Sharif University of Technology in 2011. His research interests include improving the thermal performance of buildings.

Emily Schneider is an undergraduate student of Civil and Environmental Engineering at University of Massachusetts Lowell. She participated in an NSF-funded REU program at WPI.

Aaron R. Sakulich is an Assistant Professor at WPI in the Civil and Environmental Engineering Department. He received his B.S. and Ph.D. from Drexel University in 2005 and 2010, respectively. His research interests include sustainable materials, increasing infrastructure durability, and engineering education.